# Molecular Mechanisms of Polymer Crystallization from Solution

P. Welch and M. Muthukumar

*Polymer Science and Engineering Department, Materials Research Science and Engineering Center, University of Massachusetts, Amherst, Massachusetts 01003*

(Received 10 May 2001; published 2 November 2001)

Our simulations of polymer crystallization from solutions show that (1) entropic barriers control the selection of the initial lamellar thickness, (2) growth at the crystalline interface is chain adsorption followed by crystallographic registry, and (3) lamellar thickening is a highly cooperative process requiring the mobility of all chains in the crystal. These results, especially the latter, challenge the conventional Lauritzen-Hoffman theory and its generalizations.

DOI: 10.1103/PhysRevLett.87.218302 PACS numbers: 61.41.+e, 82.35.Lr, 83.80.Ab, 87.15.Nn

Crystallization of polymers from metastable liquids and solutions is extremely complex [1–3] and its molecular mechanism is not at all understood [4,5], in spite of the rich phenomenology cultivated over 60 years of investigation. The way polymers crystallize is drastically different from that [6] of small molecules. The nucleation and growth (NG) process is recognized to be the mechanism of crystallization when a liquid of small molecules is quenched to temperatures in the metastable region. Here, crystal nuclei larger than a certain critical size are formed by thermal fluctuations, which then provide growth surfaces for further crystallization. In this small molecule case, the characteristic size of the molecule is much smaller than that of the crystal nucleus and each molecule participates in only one nucleus at a time. The situation is much more complicated for the same process involving polymers due to their topological connectivity. The ability of different portions of a single polymer molecule to participate in different initial nuclei is associated with entropic frustration and leads to incomplete crystallization whereby polymer chains fold [7] back and forth to form crystalline lamellae. The chain folding problem is in the same class [5] as the complicated protein folding problem, although much simpler in details, and requires the understanding of entropic frustration associated with chain connectivity. Availability of sensitive synchrotron radiation techniques [8–11] and molecular modeling [12–15] have spurred recent intense interest in following the mechanism of polymer crystallization.

Among the numerous challenges [1–5] faced in understanding hierarchical structures in polymer crystallization, we focus on only two issues in this Letter. (1) Independent of crystallization conditions, whether from solutions or melt, the lamellar thickness is approximately 10 nm, about 2 orders of magnitude smaller than thermodynamic estimates. Clearly, the chains should fold back and forth in the crystalline lamellae to support the experimentally observed lamellar thickness. The free energy of a folded state results from attractions among nonbonded monomers and penalties for torsional bending along the chain backbone. Different folded states of the crystalline polymer have different free energies and must be separated by barriers. In this Letter we report our modeling results on these barriers that are responsible for the spontaneous selection of lamellar thickness. (2) The problem of how a sufficiently large lamella grows further has attracted [1,4] most of the theoretical effort [16–18] in the past and a vast amount of experimental data is available. In the analytically tractable model [4,16] of Lauritzen and Hoffman (LH) and further elegant generalizations [17], the growth occurs via crossing another nucleation barrier associated with the formation of one stem of the polymer (of contour length comparable to lamellar thickness) followed by an essentially down-hill process of lateral spreading by other stems. Depending on the relative rates of nucleation of the first stems and lateral spreading, three regimes have been identified [4] and experimental data are argued [16] to be consistent with the LH theory. However, serious criticism of the LH theory lingers in the literature [1,4,18,]. In this Letter we address the molecular details of the barrier for the attachment of a stem at the growth front and what constitutes the stems. We also address the collective behavior of many chains as the growth front progresses and the lamella thickens.

Motivated by the complexity of the problem and the earlier success [13,14] of molecular modeling to provide insight into quench depth dependence of lamellar thickness, resolution of the interpretative discrepancy (spinodal mode versus NG) in the early stage of crystallization, etc., we have employed Langevin dynamics simulations to address the above two issues. To summarize our present results on polymer crystallization from dilute solutions, a nucleation and growth mechanism, not spinodal dynamics, gives birth to initial crystal nuclei (baby nuclei) in the early stages of homogeneous crystallization. Free energy barriers dictate the initial lamellar thickness. Once this baby nucleus has formed, chains diffuse to the growth front where they simultaneously adsorb and crystallographically attach. This step is not hindered by a barrier, in contradiction with the underlying assumptions of the LH theory. The newly added, folded chains undergo a rearrangement on the growth front to form stems that are commensurate with the crystal thickness at the growth front. Meanwhile, chain dynamics within the crystal result in an overall thickening of the lamella. The combined effect of

  

these events yields phenomena equivalent to experimental observations.

Our simulations employ a bead-spring united atom model to represent polymer chains, with force fields to include chain connectivity, bond angle, torsion angle, and nonbonded bead-bead interactions (Lennard-Jones of strength $\epsilon$ and range $\sigma$). The force field parameters and details are given in our earlier work [13,14]. All results are given in terms of $\epsilon$ and the equilibrium bond length $l_o$. The reduced time $t$ is given in units of $\sqrt{m\sigma^2/\epsilon}$, where $m$ is the mass of a bead.

*(1) Spontaneous selection of lamellar thickness.*—We have calculated the free energy landscape as a function of a measure, $L$, of lamellar thickness of single chains at a given quench depth and utilizing a histogram technique [19]. $L$ is the the radius of gyration along the axis parallel to the chain backbone within the crystal. The free energy $F(L)$ is estimated as $F(L) = -kT \ln(\frac{n(L)}{\mathcal{N}})$, where $n(L)$ is the number of times the system visited states between $L$ and $L + \Delta L$, $\mathcal{N}$ is the total number of states visited, and $kT$ is the Boltzmann constant times absolute temperature. Figure 1A illustrates our estimates of the free energy profiles for a 200 united atom chain ($N = 200$) at a quench depth of approximately 2 ($\Delta T/\epsilon \approx 2$). $\Delta L/l_o$ is 2. The estimate was constructed by performing nine different simulations for 60 000 reduced time units. Samples were recorded every 20 time units. Each well corresponds to a different number of stems in the crystal. For example, six, five, and four stem structures are observed for chains composed of 200 united atoms. Increasing the number of united atoms, $N$, results in the addition of more wells. Thus, the profile for $N = 300$ displays four wells corresponding to structures with four to seven stems. The minimum in $F[L]$ is observed to be near $L/l_o \approx 9$ for all chain lengths examined. This corresponds to different numbers of stems for different values of $N$. As $N$ increases, the chains increase the number of stems in the crystal to accommodate the target minimum $F[L]$ crystal thickness. However, the number of beads in each stem at this minimum is always approximately 40 (which is equivalent to $L/l_o \approx 9$). Note that the barrier between this kinetically selected thickness and other thicker lamellae is increasing prohibitively as the thickness increases. Further, we also observe the barriers in $F[L]$ between the local minima to increase with $N$. We therefore expect that at larger values of $N$ the rearrangement from one crystal thickness to the next happens with far less frequency than that illustrated in Fig. 1A. We therefore conclude that the spontaneous selection of the initial lamellar thickness is dictated by the huge free energy barrier for forming thicker lamellar (fewer stems).

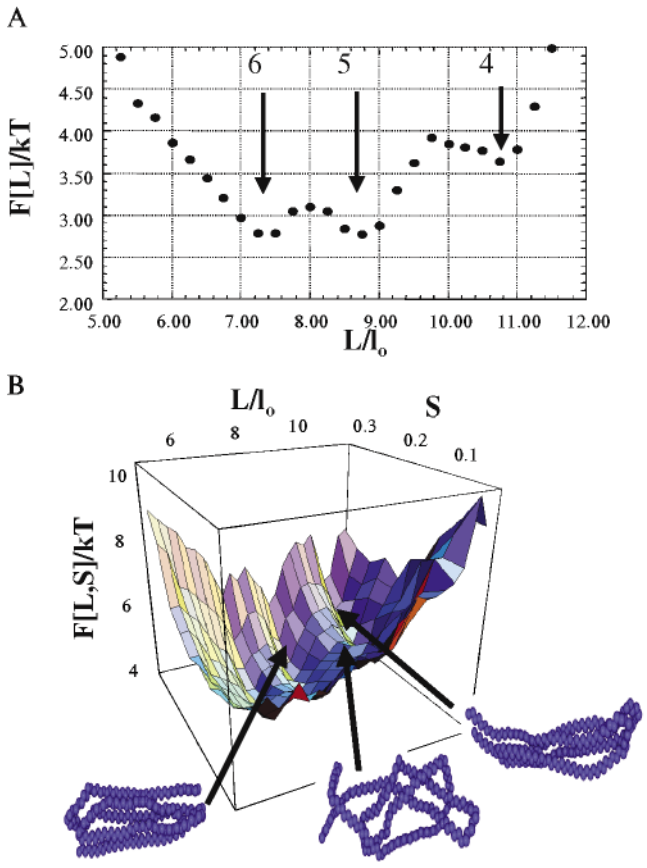


FIG. 1 (color). (A) The free energy density as a function of $L$ for $N = 200$. The numerical labels indicate the number of stems for the corresponding free energy wells. (B) The free energy density as a function of both $L$ and $S$ for $N = 200$. The snapshots indicate the ordered configurations typical of the wells and the disordered structures of the saddles.

Close examination of the simulations indicates that the chains tend to "melt" while jumping a barrier. We estimated the free energy landscape as a function of both $L$ and orientational order, $S$, to quantify this behavior. The global orientational order parameter $S = 0.5\langle 3\cos^2\phi - 1\rangle_{\text{pairs}}$ measures the degree of crystalline order in the chain folded structure, where $\phi$ is the angle between any pair of vectors that join two chain segments and $\langle\rangle_{\text{pairs}}$ indicates an average over all such vector pairs in a given chain conformation. $F[L, S]$ was approximated using a two-dimensional histogram with $n(L, S)$, the number of times the chain was observed to be in a state with a thickness between $L$ and $L + \Delta L$ and an orientational order between $S$ and $S + \Delta S$ ($\Delta S = 0.03$). Figure 1B presents our estimate of $F[L, S]$ for $N = 200$. Configurations gathered for Fig. 1A were used in this estimate. Three valleys are noted in the landscape along the $L$ axis. These correspond to the three chain folded structures reflected in Fig. 1A above. Given this landscape, there are two limiting cases for the chain to move from one valley to the next. The chain may maintain its orientational order and thereby jump the large free energy barrier required to get to the next well. Or, it may disorganize and cross the saddle of the landscape and then slide towards higher $S$ values in the new valley. The latter journey is most often observed in our simulations for single folded chains.

*(2) Mechanism of chain addition to a growing crystal and simultaneous lamellar thickening.*—We have carried

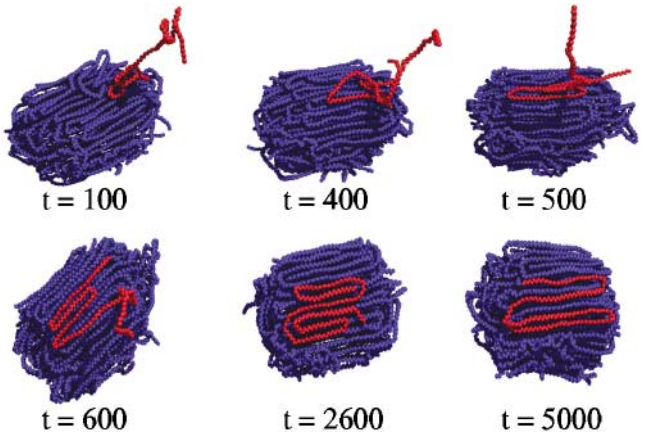


FIG. 2 (color). Representative snapshots from the simulation. The 40th chain adding to a 39 chain crystal.

out very long simulations with as many as 9000 united atoms with the following protocol. First, we placed a single chain crystal at the origin. Next, a self-avoiding random chain was placed at a random location on a sphere whose radius is 1.5 times the radius of gyration, $Rg$, of the crystal. The new system was equilibrated with the Langevin dynamics algorithm for 5000 time units. If the chain failed to add any segments to the crystal by the end of the addition period, the run was rejected and the crystal's coordinates were reset to their values at the beginning of the period. A new attempt to add a chain was then made. If the chain added to the crystal, the process was repeated by moving the crystal to the origin and adding a new self-avoiding random chain to the simulation. This procedure corresponds to the conditions of Regime I in Hoffman's nomenclature. This process was repeated until 45 chains were in the crystal, for $kT/\epsilon = 9.0$ corresponding to $\Delta T/\epsilon \approx 2.0$.

Figure 2 illustrates the addition of the 40th chain to a 39 chain crystal. The crystal reels in the chain one segment at a time, crystallographically attaching each to the growth face. This process continues until the entire chain adds to the crystal. Once adsorbed, the chain continues to rearrange until its fold length is commensurate with that of the growth face. The rate limiting step for the addition of the chain to the crystal is the diffusive contact with the surface. Once a few segments have come into contact with the crystal, the chain rapidly adds to the growth front. This suggests that there is no free energy barrier for the addition of segments or stems to the crystal. We again applied the histogram technique to approximate the free energy as a function of the number of segments added to the crystal, $F[s]$. Our estimate was obtained as above, replacing $n(L)$ with $n(s)$, a histogram reflecting the number of segments, $s$, from an incoming chain that have added to the growth front. Figure 3 clearly shows that there are no large barriers to the addition of the chain segments to the crystal. $F[s]/kT$ rapidly decreases once a few segments have added to the growth face. Some small barriers may exist,

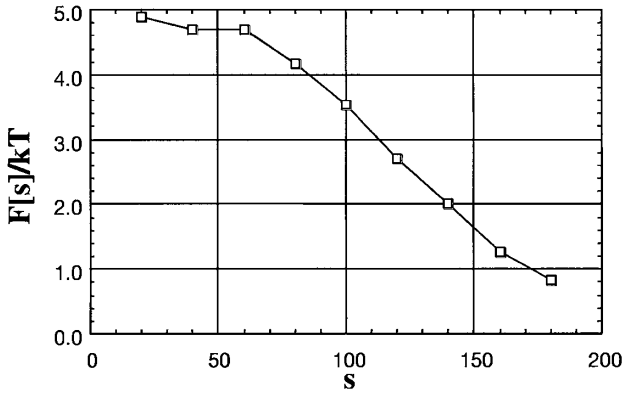


FIG. 3. Estimate of the free energy for adding new chain segments to the growth face.

corresponding to the formation of the hairpins. However, since the chains added rapidly to the growth face, relatively few samples were available for our estimate. We obtained $n(s)$ from the snapshots of the second through the 45th chain adding to the crystal. These snapshots were saved at a rate of one every 50 time units. Thus, only 4500 states were used in our approximation of $F[s]$. This limitation necessitated a broad bin width of $\Delta s = 20$ segments. Small barriers, if present, are therefore smoothed out. Our results sharply contradict the underlying assumptions of the LH theory and its generalizations mainly because these theoretical developments ignore chain mobility inside lamellae.

Chains inside crystals grown in this fashion move cooperatively. The center of mass of the crystal diffuses in space while the crystal thickens by a process of internal rearrangement. Labeling one chain in the growing structure reveals both this collective motion of the crystal and the internal reorganization, as shown in Fig. 4. Here, the oldest chain in the system is depicted at both an early and a late stage of crystal growth. The coordinate origin and an $x-y$ plane are provided for reference. In the early stages, nine other chains surround and interpenetrate the labeled chain which has arranged itself into four stems. The space

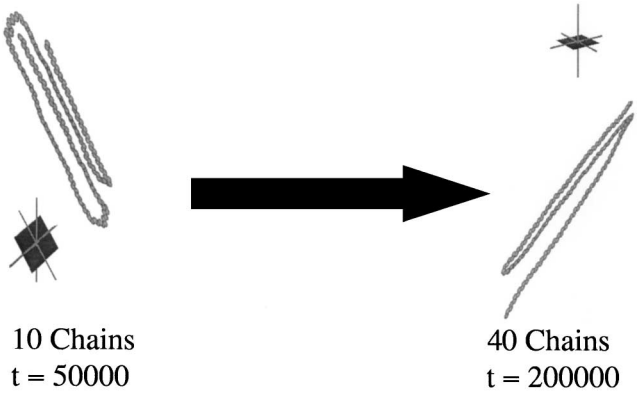


FIG. 4. Snapshots of the first chain in the midst of other chains at different stages of crystal growth.

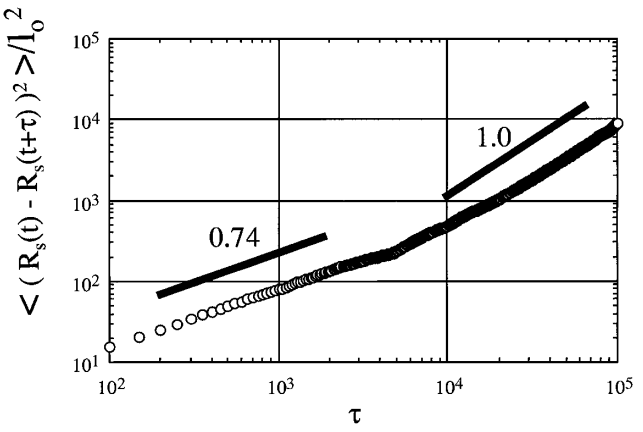


FIG. 5. The squared displacement in time for a tagged chain segment. Data shown for segment 60 of the first chain.

visible between the stems indicates a nonadjacent reentry mode for the chain segments. This suggests that the stems have a lateral mobility since the crystal began growing with this single tagged chain. Later, in the presence of 39 other molecules, the labeled chain now spans only three stems. This demonstrates that some chain segments have moved through the crystal lattice, into the fold surface, and back into the crystalline region, in accord with recent NMR data [20]. Figure 5 illustrates that two regimes are operative in the time evolution of a single segment's location. The time correlation function of the location $R_s(t)$ of a tagged segment, $\langle [R_s(t) - R_s(t + \tau)]^2 \rangle$, is proportional to $\tau$ at larger values of $\tau$, characteristic of Brownian diffusion. For smaller values of $\tau$, a new effective power law is observed: $\langle [R_s(t) - R_s(t + \tau)]^2 \rangle \propto \tau^{0.74}$. The exponent of 0.74 was obtained by averaging the behavior of eight segments of the six oldest chains in the crystal. This new law appears as a compromise between the essentially one-dimensional random walk $\{\langle [R_s(t) - R_s(t + \tau)]^2 \rangle \propto \tau^{1.0}\}$ behavior that the segments undergo within the crystal and the Rouse dynamics $\{\langle [R_s(t) - R_s(t + \tau)]^2 \rangle \propto \tau^{0.5}\}$ of the amorphous fold region.

In conclusion, Langevin dynamics simulation results reported here provide several new insights into the spontaneous selection of lamellar thickness, the nucleation mechanisms of lamellar growth, and lamellar thickening. The picture presented here challenges the underlying assumptions of LH theory and its generalizations. We therefore hope that this Letter will stimulate more extensive simulations on larger systems under varying conditions, new theoretical models, and new time resolved experiments.

This research was supported by the NSF Grant No. DMR 9970718 and the MRSEC at the University of Massachusetts.

[1] Special issue on Organization of Macromolecules in the Condensed Phase [Discuss. Faraday Soc. **68**, 7–516 (1979)].
[2] G. Strobl, *The Physics of Polymers* (Springer, New York, 1997).
[3] D. C. Bassett, *Principles of Polymer Morphology* (Cambridge University Press, Cambridge, England, 1981).
[4] K. Armitstead and G. Goldbeck-Wood, *Advances in Polymer Science* (Springer-Verlag, New York, 1992), Vol. 100.
[5] M. Muthukumar, Eur. Phys. J. E **3**, 199 (2000).
[6] V. P. Skripov, *Metastable Liquids* (Wiley, New York, 1973).
[7] K. H. Storks, J. Am. Chem. Soc. **60**, 1753 (1938); A. Keller, Philos. Mag. **2**, 1171 (1957).
[8] M. Imai *et al.,* Phys. Rev. Lett. **71**, 4162 (1993); M. Imai *et al.,* Phys. Rev. B **52**, 12 696 (1995).
[9] P. D. Olmsted *et al.,* Phys. Rev. Lett. **81**, 373 (1998).
[10] N. J. Terrill *et al.,* Polymer **39**, 2381 (1998).
[11] T. A. Ezquerra *et al.,* Phys. Rev. E **54**, 989 (1996).
[12] T. A. Kavassalis and P. R. Sundararajan, Macromolecules **26**, 4144 (1993); T. Yamamoto, J. Chem. Phys. **109**, 4638 (1998); S. Gautam, S. Balijepalli, and G. C. Rutledge, Macromolecules **33**, 9136 (2000); H. Meyer and F. Müller-Plathe, www.arXiv.org/archive/cond-mat, manuscript 0012264.
[13] C. Liu and M. Muthukumar, J. Chem. Phys. **109**, 2536 (1998).
[14] M. Muthukumar and P. Welch, Polymer **41**, 8833 (2000).
[15] J.-U. Sommer and G. Reiter, J. Chem. Phys. **112**, 4384 (2000).
[16] J. I. Lauritzen and J. D. Hoffman, J. Res. Natl. Bur. Stand. Sect. A **64**, 73 (1961); **65**, 297 (1961); J. Appl. Phys. **44**, 4340 (1973); J. D. Hoffman and R. L. Miller, Polymer **38**, 3151 (1997).
[17] E. A. DiMarzio, J. Chem. Phys. **47**, 3451 (1967); I. C. Sanchez and E. A. DiMarzio, J. Chem. Phys. **55**, 893 (1971); Macromolecules **4**, 677 (1971); J. Res. Natl. Bur. Stand. **76A**, 213 (1972); E. A. DiMarzio and C. M. Guttman, J. Appl. Phys. **53**, 6581 (1982); E. A. DiMarzio and E. Passaglia, J. Chem. Phys. **87**, 4901 (1987); **87**, 4908 (1987).
[18] J. J. Point, Macromolecules **12**, 770 (1979); D. Sadler and G. H. Gilmer, Polymer **25**, 1446 (1984); Phys. Rev. Lett. **56**, 2708 (1986); Phys. Rev. B **38**, 5684 (1988); G. Allegra, J. Chem. Phys. **66**, 5453 (1977); G. Allegra and S. V. Meille, Phys. Chem. Chem. Phys. **1**, 5179 (1999).
[19] S. Kumar *et al.,* J. Comput. Chem. **13**, 1011 (1992).
[20] K. Schmidt-Rohr and H. W. Spiess, Macromolecules **24**, 5288 (1991).